

THE GEOMETRY OF GENERIC SLIDING BIFURCATIONS

M. R. JEFFREY AND S. J. HOGAN *

Abstract. Using the singularity theory of scalar functions, we derive a classification of sliding bifurcations in piecewise-smooth flows. These are global bifurcations which occur when distinguished orbits become tangent to surfaces of discontinuity, called switching manifolds. The key idea of the paper is to attribute sliding bifurcations to singularities in the manifold's projection along the flow, namely to points where the projection contains folds, cusps, and two-folds (saddles and bowls). From the possible local configurations of orbits we obtain sliding bifurcations.

In this way we derive a complete classification of generic one-parameter sliding bifurcations at a smooth codimension one switching manifold in n -dimensions for $n \geq 3$. We uncover previously unknown sliding bifurcations, all of which are catastrophic in nature. We also describe how the method can be extended to sliding bifurcations of codimension two or higher.

Key words. Sliding, Filippov, discontinuity, bifurcation, singularity, grazing

AMS subject classifications. 34C23,37G05,37G10,37G15

1. Introduction. Bifurcation theory for systems of ordinary differential equations describes how smooth variations of parameter values can, through topological changes, cause sudden changes in dynamics. This paper considers the effect of discontinuous variation in the differential equations themselves, which give rise to the discontinuity-induced bifurcations [6] of piecewise-smooth dynamical systems.

We will study bifurcations that affect individual orbits as a single parameter varies. The Flowbox Theorem [23] shows that in the neighbourhood \mathcal{U} of a point where a flow is smooth and non-vanishing, all orbits are smoothly equivalent. We cannot, therefore, study the global bifurcation of a distinguished orbit Γ passing through \mathcal{U} by studying dynamics in \mathcal{U} alone. The same is not true if the flow is piecewise-smooth in \mathcal{U} with a discontinuity along a surface Σ . Then parameter variation can lead to local changes in the intersection between Γ and Σ . If the change involves orbits which are confined to 'slide' along the discontinuity then this is called a *sliding bifurcation*. Provided that the discontinuity occurs along a smooth codimension one *switching manifold*, we will show that all one parameter sliding bifurcations in \mathbb{R}^n are equivalent to just 8 cases, each of which occur generically in \mathbb{R}^2 or \mathbb{R}^3 , and of which only four are already known.

Piecewise-smooth systems are widespread in applications such as engineering, economics, medicine, biology and ecology. Problems with impacts, friction, or switching are piecewise-smooth. For recent accounts of such systems see [6, 21, 34]. The systems we consider are expressible in the form

$$\dot{x} = f(x, t; \mu) \tag{1.1}$$

where $x \in \mathbb{R}^n$ is a state vector, $\mu \in \mathbb{R}$ is a parameter (which may more generally be a vector), and $\dot{x} = dx/dt$ with $t \in \mathbb{R}$. The function $f : \mathbb{R}^{n+2} \rightarrow \mathbb{R}^n$ is piecewise-smooth, with discontinuities occurring across a hypersurface through phase space, called the switching manifold.

To fully define solutions of (1.1), a rule must be given to prescribe the dynamics at the switching manifold. If the rule is to apply a map from one point on the manifold to

*Bristol Centre for Applied Nonlinear Mathematics, Department of Engineering Mathematics, University of Bristol BS8 1TR. (contact email: mike.jeffrey@bristol.ac.uk). This work was supported by the EPSRC grant EP/E032249/1

another, the solution $x(t)$ can be discontinuous, leading to hybrid or impact systems [6]. The subject of this paper is systems where the solution $x(t)$ remains continuous, but can be non-unique at the manifold [10]. A local form for such systems is

$$\dot{x} = f(x; \mu) = \begin{cases} f^+(x; \mu) & \text{if } h(x) > 0, \\ f^-(x; \mu) & \text{if } h(x) < 0, \end{cases} \quad (1.2)$$

where $h(x) = 0$ implicitly defines the switching manifold. Each of the vector fields f^+ and f^- is smooth and defined for all x . At $h = 0$, trajectories either cross through the switching manifold or slide along it, see Fig. 1.1.

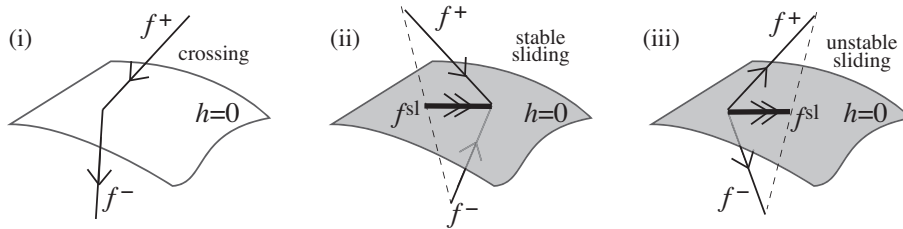


FIG. 1.1. Piecewise-smooth vector fields in regions of (i) crossing, (ii) stable sliding, (iii) unstable sliding. The sliding vector field f^{sl} (double arrows) is a convex combination of f^+ and f^- . This formalism is due to Filippov [10] and Utkin [32], and is said to define a Filippov system.

Sliding trajectories are solutions of

$$\dot{x} = f^{\text{sl}} \equiv (1 - \lambda)f^+ + \lambda f^-, \quad \text{where } \lambda = \frac{\mathcal{L}_{f^+}h}{(\mathcal{L}_{f^+}h - \mathcal{L}_{f^-}h)}, \quad (1.3)$$

defined on $h = 0$ wherever $(\mathcal{L}_{f^+}h)(\mathcal{L}_{f^-}h) < 0$, where \mathcal{L}_f denotes the Lie derivative $\mathcal{L}_f \equiv f \cdot \frac{d}{dx}$ along the flow of f , where $\frac{d}{dx}$ is the gradient. (Later we will also make use of the n -th derivative $\mathcal{L}_f^n \equiv (\mathcal{L}_f)^n$). The sliding vector field f^{sl} is a convex combination of f^+ and f^- , with λ defined such that f^{sl} is always tangent to the manifold.

DEFINITION 1.1. An **orbit segment** is a smooth curve which is a trajectory of (1.2) in the regions $h > 0$ or $h < 0$. A **sliding segment** is a smooth curve which is a trajectory of (1.3) on $h = 0$. An **orbit** is a continuous curve $x(t)$ that is a concatenation of orbit segments and sliding segments.

DEFINITION 1.2. A **topological equivalence** between Filippov systems $F = \{f, f^{\text{sl}}\}$ and $F' = \{f', f'^{\text{sl}}\}$, is a homeomorphism on \mathbb{R}^n that sends orbits of F to orbits of F' , preserving orbit segments, sliding segments, and time direction.

For more detailed definitions see [10, 20]. Note this is stronger than a definition given in [1] because orbits, not just segments, are preserved. This is essential in the present paper, as it respects the intersection of orbits with the switching manifold.

Orbits are then continuous, but need not be differentiable (following Filippov's convention [10]). Where $\lambda < 0$ or $\lambda > 1$ in (1.3) we have $(\mathcal{L}_{f^+}h)(\mathcal{L}_{f^-}h) > 0$, then orbit segments either side of $h = 0$ can be concatenated to form an orbit that crosses the switching manifold (Fig. 1.1(i)).

Orbit segments can also be concatenated with sliding segments. Orbits with sliding segments are non-unique in the sense that infinitely many orbits pass through any point in the sliding region. Sliding regions on $h = 0$ satisfy $0 < \lambda < 1$, and come in two forms. If $\mathcal{L}_{f^+}h < 0 < \mathcal{L}_{f^-}h$ then the sliding is *stable* (Fig. 1.1(ii)), orbits reach the manifold in finite time and follow the sliding vector field f^{sl} along it. If

$\mathcal{L}_{f^+}h > 0 > \mathcal{L}_{f^-}h$ then the sliding is *unstable* (Fig. 1.1(iii)), orbits follow the sliding vector field on the switching manifold, but also escape into $h > 0$ and $h < 0$. The stability type can be interchanged by reversing the arrow of time. Unstable sliding, sometimes called ‘escaping’, has historically received less attention, but will play a vital role in what follows.

Boundaries between sliding and crossing occur where $\mathcal{L}_{f^+}h$ or $\mathcal{L}_{f^-}h$ vanish, implying that f^+ or f^- in (1.2) are tangent to the switching manifold. Since $\mathcal{L}_{f^+}h = 0 \Rightarrow \lambda = 0$, and $\mathcal{L}_{f^-}h = 0 \Rightarrow \lambda = 1$, from (1.3) we have boundary conditions for f^{sl} ,

$$\begin{cases} f^{\text{sl}} = f^+ & \text{if } \mathcal{L}_{f^+}h = 0, \\ f^{\text{sl}} = f^- & \text{if } \mathcal{L}_{f^-}h = 0. \end{cases} \quad (1.4)$$

A tangency is called *visible* or *invisible* depending on whether orbits locally curve away from, or towards, the manifold, as illustrated in Fig. 1.2(i-ii). It is also possible for sliding segments to be tangent to the sliding region’s boundary, and these similarly are referred to as either visible or invisible as shown in Fig. 1.2(iii-iv). When a tangency occurs in the vector field we say that an orbit there is *grazing*.

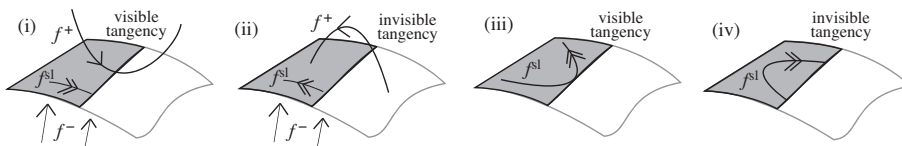


FIG. 1.2. *Tangencies in a piecewise-smooth system. Visible (i) and invisible (ii) tangencies form the boundaries between sliding (shaded) and crossing (unshaded). Tangencies between the sliding vector field and the sliding region’s boundary can also be visible (iii) or invisible (iv).*

Hence a grazing orbit is a nongeneric trajectory which, under perturbation, loses or gains points of intersection with the manifold. This leads to the observation that orbits in Filippov systems can undergo a variety of topological changes, called *sliding bifurcations*. Originally proposed in the Russian literature [9], until recently only the cases sketched in Fig. 1.3 were known [20]. The aim of this paper is to give a systematic classification of sliding bifurcations, and this will reveal hitherto unknown cases where unstable sliding plays a vital role.

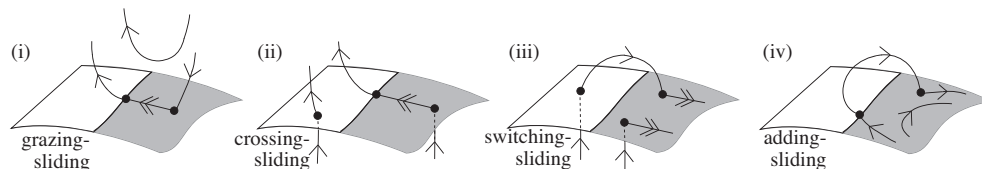


FIG. 1.3. *Four sliding bifurcations: (i) grazing-sliding, (ii) crossing-sliding, (iii) switching-sliding and (iv) adding-sliding [6]. In each case the sliding region (shaded) is stable. These have been found, for example, in relay circuits, dry-friction oscillators, and predator-prey models [6, 7, 8, 20].*

We will now define sliding bifurcations and introduce the central result of the paper, Theorem 1.4. The different sliding bifurcations will be described in section 5.

A bifurcation occurs in a system if an arbitrarily small perturbation gives topologically nonequivalent orbits according to Definition 1.2. If topological equivalence is lost due to a change in a particular orbit’s intersection with the switching manifold, we say it undergoes a sliding bifurcation, defined as follows.

DEFINITION 1.3. *A distinguished orbit $x(t; \mu)$ of (1.2)-(1.3) undergoes a **sliding bifurcation** at $x = \mu = 0$, if the vector field $f^+(0; 0)$ or $f^-(0; 0)$ is tangent to the switching manifold, and an arbitrarily small perturbation in μ gives a topologically nonequivalent orbit. We will refer to the μ -family of orbits as an **unfolding** of the sliding bifurcation.*

There are three types of tangency that will feature in this paper. The simplest is a quadratic contact between the vector field and the manifold, as in Fig. 1.2(i-ii), called a *fold*. The next is a cubic contact, called a *cusp*, which is responsible for the sliding tangencies shown in Fig. 1.2(iii-iv). The third is a quadratic contact to both sides of the manifold, called a *two-fold*. We need consider no higher order tangencies because of the following theorem, which we prove in section 5.7.

THEOREM 1.4. *A generic one-parameter sliding bifurcation in \mathbb{R}^n for any $n \geq 3$ occurs either at a fold, cusp, or two-fold.*

The rest of this paper is organised as follows. We conclude the present section with a brief discussion of what is meant by the term ‘sliding bifurcation’. In section 2, we properly define the tangencies that occur generically in Filippov systems in \mathbb{R}^2 and \mathbb{R}^3 . In section 3 we give an explicit local form for Filippov systems as straight vector fields either side of a curved switching manifold. This leads to the key idea of the paper, in section 4, to derive normal forms for the manifold from singularity theory [2, 3, 11], and then add dynamics to derive sliding bifurcations in each setting. This is an alternative to previous uses of singularity theory in nonsmooth systems, where normal forms have been derived for divergent diagrams [22, 28], and for vector fields tangent to a switching manifold [30], or to a boundary [26, 33].

The main results of the paper follow in section 5, where we first derive an unfolding around nongeneric trajectories, and use it to find a complete classification of one-parameter sliding bifurcations. In section 5.7 we show that these form the building blocks for all one-parameter sliding bifurcations in \mathbb{R}^n , and some codimension two sliding bifurcations are described in section 5.8. In the Appendix we show that our geometric approach reproduces the normal forms for vector fields at flat switching manifolds, which are equivalent to those provided by other authors, and thus applies to generic Filippov systems.

1.1. What is a sliding bifurcation? A key insight behind Theorem 1.4 is that the topological instability constituting a sliding bifurcation is localized to the neighbourhood of the switching manifold [8]. Consider a distinguished orbit entering the neighbourhood \mathcal{U} of a point on the switching manifold. The orbit is distinguished by global conditions, but the changes it can undergo relative to the manifold, in \mathcal{U} , depend only on the configurations of orbits that are possible in \mathcal{U} . As the orbit explores these different configurations it undergoes sliding bifurcations, and the same ones therefore affect, for example: (i) an unstable manifold, and (ii) a periodic orbit, shown in Fig. 1.4. Thus sliding bifurcations are *local* mechanisms for *global* bifurcations.

One way of describing this is to let $x(t; \mu)$ denote, for each $\mu > 0$, an orbit of (1.2)-(1.3) which is an organising centre of the global dynamics. Let this graze at $x = 0$ when $\mu = 0$. Define a map $T_\mu : \mathbb{R}^n \mapsto \mathbb{R}^n$ that induces a map on the vector fields $f(x; \mu)$ and $f^{\text{sl}}(x; \mu)$, given in the neighbourhood of $x = 0$ by

$$T_\mu (f(x; 0), f^{\text{sl}}(x; 0)) = \{f(x; \mu), f^{\text{sl}}(x; \mu)\}. \quad (1.5)$$

Assume that T_μ does not induce any bifurcation of f^+ or f^- . Nevertheless, typically the orbit $x(t; \mu)$ is no longer grazing for $\mu \neq 0$, and thus has undergone a sliding bifurcation by Definition 1.3. If we now apply the inverse map T_μ^{-1} to the vector

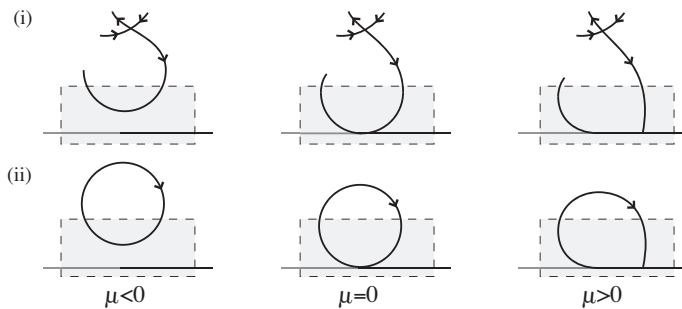


FIG. 1.4. Sliding bifurcations as a local mechanism for global bifurcations. As μ changes a sliding segment is created in: (i) the stable manifold to a saddle, and (ii) a periodic orbit. The topological change is the same: locally (grey box) the phase portraits for (i) and (ii) are equivalent.

field, it returns locally to the form $\{f(x; 0), f^{\text{sl}}(x; 0)\}$, but the orbit $x(t; \mu)$ is defined globally, so it will map to some new orbit whose local expression is $\tilde{x}(t; \mu)$ and satisfies $\tilde{x}(t; 0) = x(t; 0)$. The sliding bifurcation then unfolds *locally* as a μ -family of orbits $\tilde{x}(t; \mu)$ in the unchanging vector field given by $\{f(x; 0), f^{\text{sl}}(x; 0)\}$. We will use such μ -families in an unchanging vector field to unfold the sliding bifurcations in section 5.

2. Singularities and the vector field. In this section we introduce the tangencies of piecewise-smooth vector fields that are generic in \mathbb{R}^3 , as proven in [30]. Because we are interested only in tangencies between the vector field and the manifold, let us assume that f^+ and f^- are linearly independent throughout the local region of interest. This implies that $f^\pm \neq 0$ and, from (1.3), that $f^{\text{sl}} \neq 0$.

The simplest tangency is a quadratic contact between the switching manifold and *one* of the vector fields f^\pm . Without loss of generality let us choose a tangency with f^+ , which occurs where $\mathcal{L}_{f^+}h = 0$, which is quadratic if $\mathcal{L}_{f^+}^2h \neq 0$. Depending on the sign of $\mathcal{L}_{f^+}h$ the tangency is visible or invisible (Fig. 1.2(i-ii)), and since f^- is not tangent to $h = 0$ we have $\mathcal{L}_{f^-}h \neq 0$. We call a point where these conditions are satisfied a *fold*. It is generic in \mathbb{R}^n for $n \geq 2$, and defined as:

DEFINITION 2.1. At a fold: $\mathcal{L}_{f^+}h = 0$, $\mathcal{L}_{f^+}^2h \neq 0$, $\mathcal{L}_{f^-}h \neq 0$, and the fold is:

1. visible if $\mathcal{L}_{f^+}^2h > 0$,
2. invisible if $\mathcal{L}_{f^+}^2h < 0$.

The contact between the vector field and the manifold is cubic if $\mathcal{L}_{f^+}^2h$ also vanishes and $\mathcal{L}_{f^+}^3h \neq 0$. Then f^+ and, by (1.4), f^{sl} , are tangent to the set of fold points where $\mathcal{L}_{f^+}h = 0$. The signs of $\mathcal{L}_{f^+}^3h$ and $\mathcal{L}_{f^-}h$ determine whether the tangency of f^{sl} is visible or invisible (Fig. 1.2(iii-iv)). We call a point where these conditions are satisfied a *cusp*, defined as:

DEFINITION 2.2. At a cusp: $\mathcal{L}_{f^+}h = \mathcal{L}_{f^+}^2h = 0$, $\mathcal{L}_{f^+}^3h \neq 0$, $\mathcal{L}_{f^-}h \neq 0$, and the vectors $\frac{d}{dx}h$, $\frac{d}{dx}\mathcal{L}_{f^+}h$, $\frac{d}{dx}\mathcal{L}_{f^+}^2h$, are linearly independent. The cusp is:

1. visible if $(\mathcal{L}_{f^+}^3h)(\mathcal{L}_{f^-}h) < 0$,
2. invisible if $(\mathcal{L}_{f^+}^3h)(\mathcal{L}_{f^-}h) > 0$.

The fold and cusp lie on the boundary of stable sliding if $\mathcal{L}_{f^-}h > 0$ and of unstable sliding if $\mathcal{L}_{f^-}h < 0$ (recall Fig. 1.1 for the types of stability). If a quadratic contact occurs between the manifold and *both* of the vector fields f^+ and f^- at the same

point, then $\mathcal{L}_{f^+}h = \mathcal{L}_{f^-}h = 0$ but the second derivatives are nonzero. Thus we have a fold with respect to both f^+ and f^- , each of which may be visible or invisible, and we call such a point a *two-fold*, defined as:

DEFINITION 2.3. *At a two-fold: $\mathcal{L}_{f^+}h = \mathcal{L}_{f^-}h = 0$, $\mathcal{L}_{f^\pm}^2h \neq 0$, and the vectors $\frac{d}{dx}h$, $\frac{d}{dx}\mathcal{L}_{f^+}h$, $\frac{d}{dx}\mathcal{L}_{f^-}h$, are linearly independent. The two-fold is:*

1. visible if $\mathcal{L}_{f^+}h > 0$ and $\mathcal{L}_{f^-}h < 0$,
2. invisible if $\mathcal{L}_{f^+}h < 0$ and $\mathcal{L}_{f^-}h > 0$,
3. visible-invisible if $(\mathcal{L}_{f^+}h)(\mathcal{L}_{f^-}h) > 0$.

Given Theorem 1.4, the conditions in definitions 2.1-2.3 are necessary and sufficient for the existence of one-parameter sliding bifurcations. To find what those bifurcations look like, we will begin by finding an explicit local approximation for the piecewise-smooth system.

3. Local piecewise-straightening. Having fixed f^+ and f^- to be linearly independent, let us now consider them to lie along the axes of a coordinate system $x = (x_1, x_2, x_3)$ in \mathbb{R}^3 , so that the vector field in (1.2) becomes simply

$$\dot{x} = f(x) = \begin{cases} f^+ = (1, 0, 0) & \text{if } h(x) > 0, \\ f^- = (0, 1, 0) & \text{if } h(x) < 0, \end{cases} \quad (3.1)$$

hence its Lie derivative is given by $\mathcal{L}_f = \mathcal{L}_{f^+} \equiv \frac{\partial}{\partial x_1}$ for $h > 0$, and $\mathcal{L}_f = \mathcal{L}_{f^-} \equiv \frac{\partial}{\partial x_2}$ for $h < 0$. We can reverse time in $h > 0$ or $h < 0$ by changing the signs of f^+ or f^- . We can also extend this to \mathbb{R}^n for $n > 3$, by adding zeros beyond the third component.

It remains to derive typical forms of h in such a system. Letting the switching manifold $h = 0$ be a general curved surface, we will relate tangencies in the system to the manifold's geometry. Moreover, in the Appendix we show that previous authors' normal forms for piecewise-smooth vector fields with folds, cusps, or two-folds [10, 20, 30], are equivalent to (3.1) with appropriate forms of h which we find in section 4.

Let us now consider the form of the switching manifold. If there is a fold or cusp at $x = 0$ in (3.1), then applying the Lie derivatives for (3.1) to Definitions 2.1-2.2, we have $\partial h(0)/\partial x_2 \neq 0$. Then we can find coordinates $x = (x_1, x_2, x_3)$ where $h(x) = x_2 + V(x)$, given $\partial V(0)/\partial x_2 = 0$. To lowest order in x_2 (for small x) then,

$$h(x_1, x_2, x_3) = x_2 + V(x_1, x_3). \quad (3.2)$$

If instead there is a two-fold at $x = 0$, then applying the Lie derivatives for (3.1) to Definition 2.3 shows that the coordinate axes x_1 and x_2 lie in the tangent plane of the switching manifold. Thus the only nonvanishing first derivative of h is $\partial h/\partial x_3 \neq 0$, and to lowest order in x_3 (for small x) we can write

$$h(x_1, x_2, x_3) = x_3 + V(x_1, x_2) \quad (3.3)$$

where $\partial V(0)/\partial x_3 = 0$. In the following section we will use results from singularity theory to find local expressions for the function V .

4. Singularity theory and the switching manifold. We now introduce some standard results of singularity theory applied to smooth surfaces. We cover only the ideas required for this paper, and refer the reader to [2, 3, 11] for particularly readable accounts of the precise statements and theory behind them.

A scalar-valued function $V(u, a)$ of a variable $u \in \mathbb{R}^p$ and a parameter $a \in \mathbb{R}^q$, can be characterised by locally classifying its stationary points where the gradient

dV/du vanishes. For a function V with a nondegenerate stationary point at $u = 0$, the Morse Lemma [24] states that we can find local coordinates $u = (u_1, u_2, \dots, u_n)$ in which $V(u, a) = V(u) = \pm \frac{1}{2}u_1^2 \pm \frac{1}{2}u_2^2 \dots \pm \frac{1}{2}u_n^2$. The set $h = 0$ of a function $h(u, v) = v + V(u)$, for $v \in \mathbb{R}$, then has a fold singularity in the space of (u, v) when projected along any of the coordinate axes of u . The zero set of h with a fold along u_1 is illustrated in Fig. 4.1(i), plotted in coordinates $(x_1, x_2) = (u_1, v)$. Folds along u_1 and u_2 are illustrated in Fig. 4.1(iii)-(iv) in the space $(x_1, x_2, x_3) = (u_1, u_2, v)$.

A stationary point is degenerate if the Hessian determinant vanishes, so $|d^2V/du^2| = dV/du = 0$. At a degenerate stationary point an invertible coordinate transformation can typically be found to express V in a ‘normal form’, which belongs to a parameterised family of functions called a universal unfolding. The universal unfolding displays the nondegenerate components making up the degeneracy over the space of u , in which, as parameters vary, sets of nondegenerate stationary points emanate from the degeneracies. A universal unfolding is structurally stable, that is, the pattern of stationary points and degeneracies persist under small perturbations to the unfolding.

For a scalar function V with a degenerate stationary point $dV(0)/du = d^2V(0)/du^2 = 0 \neq d^3V(0)/du^3$, we can find a local coordinate $u = u_1$ such that $V(u_1) = \frac{1}{3}u_1^3$. This is structurally unstable. The normal form of its universal unfolding is $V(u_1, a) = \frac{1}{3}u_1^3 + au_1$, where a is a real parameter, so that $\partial^2V(0,0)/\partial u_1 \partial a \neq 0$ ensures structural stability [24]. For a function $h(u, v, a) = v + V(u, a)$, the level sets of h have curves of fold singularities when projected along the u_1 -coordinate axis in the space of (u_1, v, a) , except at $u_1 = a = 0$, where the projection has a cusp at which two folds meet. This is illustrated in Fig. 4.1(ii) in coordinates $(x_1, x_2, x_3) = (u_1, v, a)$.

In general, the dimension of the parameter a in $V(x, a)$ is the smallest possible for the unfolding to be stable, called the *codimension*. Only the singularities in Fig. 4.1 (of codimension 0 or 1) will feature in this paper. We discuss the role of higher codimension singularities in sliding bifurcations in sections 5.7-5.8.

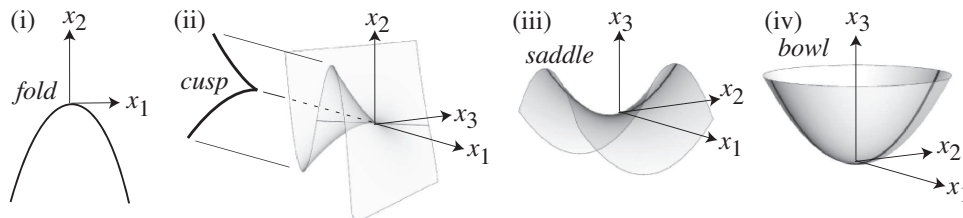


FIG. 4.1. *Generic singularities of the function $h = 0$, for: (i) the fold $h = x_2 + \frac{1}{2}x_1^2$; (ii) the cusp $h = x_2 + (\frac{1}{3}x_1^3 + x_3x_1)$; the two-fold, which is either (iii) a saddle $h = x_3 + (\frac{1}{2}x_1^2 - \frac{1}{2}x_2^2)$ or (iv) a bowl $h = x_3 + (\frac{1}{2}x_1^2 + \frac{1}{2}x_2^2)$. Writing $h(u, v, a) = v + V(u, a)$, the x -coordinates correspond to: (i) $(x_1, x_2) = (u_1, v)$, (ii) $(x_1, x_2, x_3) = (u_1, v, a)$, and (iii-iv) $(x_1, x_2, x_3) = (u_1, u_2, v)$.*

These ideas are of use in dynamical systems if a problem can be reduced to considering a scalar function, for example, in a gradient dynamical system $\dot{u} = dV(u)/du$, an unfolding $V(u_1, a) = \frac{1}{3}u_1^3 + au_1$ would describe a saddle-node bifurcation [19]. The central idea of the present paper is to exploit (3.2)-(3.3), whereby the switching manifold is expressed as the zero set of a scalar function $h = v + V$. Then at a fold or cusp, from (3.2), the switching manifold is given by $h(x_1, x_2, x_3) = x_2 + V(x_1, x_3) = 0$. In the straightened vector field of (3.1) there are no dynamics in the x_3 direction, and hence x_3 behaves like a parameter, so we can map (u_1, v) onto the coordinates (x_1, x_2) as in Fig. 4.1(i), or map (u_1, v, a) onto the coordinates (x_1, x_2, x_3) as in Fig. 4.1(ii). Transformations on the coordinates x_1 only are sufficient to put V into either

of the normal forms $V = \pm \frac{1}{2}x_1^2$ or $V = \frac{1}{3}x_1^3 + x_3x_1$, since x_3 can be chosen arbitrarily because $\dot{x}_3 = 0$ in (3.1). It is easily verified, by applying the Lie derivatives for (3.1), that the straightened vector field with

$$h(x_1, x_2) = x_2 \pm \frac{1}{2}x_1^2 \quad (4.1)$$

describes a fold in the vector field consistent with Definition 2.1, and with

$$h(x_1, x_2, x_3) = x_2 + \frac{1}{3}x_1^3 + x_3x_1 \quad (4.2)$$

describes a cusp in the vector field consistent with Definition 2.2.

At a two-fold, according to (3.3), we can express the switching manifold as $h(x_1, x_2, x_3) = x_3 + V(x_1, x_2) = 0$. If we simply let $(u_1, u_2, v) = (x_1, x_2, x_3)$, then the vector field in (3.1) would lie tangent to the fold curves on $h = 0$ and violate the non-degeneracy conditions in Definition 2.3. Instead we map a linear combination of u_1 and u_2 to x_1 and x_2 , obtaining a general expression for V as $V = c_1x_1^2 + c_2x_2^2 + c_3x_1x_2$. We are free to choose the constants c_i to give

$$h(x_1, x_2, x_3) = x_3 + \frac{1}{2}\alpha x_1^2 - \frac{1}{2}\beta x_2^2 + x_1x_2, \quad (4.3)$$

where the parameters α and β describe the alignment of the folds to the coordinate axes, and must be nonzero. Applying the Lie derivatives for (3.1), it is easily seen that the straightened vector field in (3.1), with V given by (4.3), describes a two-fold consistent with Definition 2.3.

5. Sliding bifurcations. This section concerns the dynamics implied by the local geometry. We have derived a local expression in which the vector field is straight, (3.1), while the switching manifold is curved and specified by one of (4.1)-(4.3). In this section we will characterise the flow by finding a surface comprised of a generic family of orbits. The surface will be expressed implicitly as a function $\psi(x) = 0$, and describes the typical shape of orbits in the piecewise-smooth flow. By considering how the surfaces $\psi = 0$ and $h = 0$ intersect, we can study how orbits lose or gain points of intersection with the switching manifold near grazing.

In general, if a scalar function $\psi(x)$ in \mathbb{R}^3 satisfies $\mathcal{L}_f\psi(x) = 0$, then a surface defined by $\psi(x) = 0$ consists of a one-parameter family of orbits of a system $\dot{x} = f$ where $f \neq 0$. For (3.1), a suitable scalar function is

$$\psi(x) = \rho(x_3) - x_i + h(x) - h(x)g(x), \quad \text{with } g = \frac{\mathcal{L}_f(h - x_i)}{\mathcal{L}_f h}, \quad (5.1)$$

where ρ is a smooth function and g is a piecewise-constant (as we show in (5.3) below). The coordinate x_i is the x component preceding V in each of the expressions of the form $h = x_i + V$ given by (4.1)-(4.3). The surface $\psi = 0$ is piecewise-smooth. When $\rho = 0$, it contains an orbit intersecting the origin, and therefore $\psi = 0$ is an unfolding of a sliding bifurcation as defined in Definition 1.3.

The surface $\psi = 0$ is comprised of a family of orbits in each of the vector fields f^+ and f^- , which have a common intersection on $h = 0$. Generically, the portions of $\psi = 0$ in $h > 0$ and $h < 0$ will each be transverse to $h = 0$. This implies that $d\psi/dx$ and dh/dx must be linearly independent. Then the intersection between $\psi = 0$ and the switching manifold $h = 0$ is a smooth curve $x_i = \rho(x_3)$, hence ρ determines the shape of the surface $\psi = 0$. We parameterize this intersection curve as $x_0(\mu)$ for $\mu \in \mathbb{R}$, and call points $x = x_0(\mu)$ the *impact coordinates*. They are found by solving

$$h(x_0) = 0 \quad \text{and} \quad \psi(x_0) = 0. \quad (5.2)$$

We will use the impact coordinates x_0 as initial data for orbits in the unfolding.

The piecewise-constant g must be evaluated on each side of the switching manifold. On a given side, if grazing occurs then $\mathcal{L}_f x_i = 0$ and $g = 1$, otherwise we must have $\mathcal{L}_f(h - x_i) = 0$ over a neighbourhood of $x = 0$, giving $g = 0$. Therefore

$$g = \begin{cases} 1 & \text{if } \mathcal{L}_f x_i = 0, \\ 0 & \text{if } \mathcal{L}_f(h - x_i) = 0, \end{cases} \quad \text{at } x = 0. \quad (5.3)$$

Note that only one of the two is possible on each side of the manifold.

In the remainder of this section we make explicit the unfoldings $\psi = 0$ given by (5.1). In this way we classify and unfold the one parameter sliding bifurcations that are possible in the neighbourhood of the singularities in section 4. The reader may find it useful also to refer to Fig. 6.1 in the Appendix, where we reproduce these results for a flat switching manifold.

5.1. Sliding bifurcation at a visible fold: grazing case. Consider the vector field in (3.1) with switching manifold $h(x) = x_2 + \frac{1}{2}x_1^2 = 0$ from (4.1). By Definition 2.1.1, this represents a visible fold. By setting $\rho = x_3$ in (5.1) we obtain an unfolding of the *sliding bifurcation at a visible fold*, given by $\psi = 0$ where

$$\begin{aligned} \psi(x) &= x_3 - x_2 + h(x)\Theta[-h(x)], \\ \text{and } h(x) &= x_2 + \frac{1}{2}x_1^2, \end{aligned} \quad (5.4)$$

where Θ is the unit step function $\Theta[h] = \frac{1}{2}(1 + \text{sgn}[h])$. We have simplified (5.4) using the identity $\Theta[h] = 1 - \Theta[-h]$. This unfolding is shown in Fig. 5.1(i). We will now describe this figure, and remind the reader that the vector field f^- in $h < 0$ is vertical and points toward the switching manifold (for clarity the arrows of f^- are not shown in Fig. 5.1(i)). Note that the sliding region is stable because $\mathcal{L}_f h > 0$.

Orbits cross the switching surface $h = 0$ where $x_1 > 0$, and slide where $x_1 < 0$. Sliding orbits (double arrows) flow towards the fold (as implied by the conditions in (1.4)), then escape into $h > 0$. The segments of orbits leaving the switching manifold at the fold form a surface given by $\psi_{\text{sl}} = 0$, where

$$\psi_{\text{sl}}(x) = -x_2 + h(x)\Theta[-h(x)], \quad x_1 \geq 0. \quad (5.5)$$

This is the *sliding separatrix* that separates orbits with sliding dynamics from those with crossing dynamics. The solution of $\psi_{\text{sl}} = 0$ is simply $x_2 = 0$ for $h > 0$ (the section of horizontal plane in Fig. 5.1(i)) and $x_1 = 0$ for $h < 0$, and is the nongeneric zero level surface of (5.1) with $\rho = 0$, whose intersection with $h = 0$ is the fold.

Using (5.2), we find that impact points in the unfolding satisfy $0 = x_3 + \frac{1}{2}x_1^2$. If we parameterize this curve as $x_0(\mu) = (\pm\sqrt{-2\mu}, \mu, \mu)$, then μ labels a family of orbits originating in $h > 0$. The nongeneric orbit at $\mu = 0$ grazes the manifold, see Fig. 5.1(i). This implies a sliding bifurcation: for $\mu > 0$, each orbit is a smooth trajectory in $h > 0$, and for $\mu < 0$, each orbit impacts on the curve $x_0(\mu) = (-\sqrt{-2\mu}, \mu, \mu)$. We call this the *grazing case* of the sliding bifurcation at a visible fold. See also Fig. 6.1.1, where this is illustrated for a flat switching manifold. It describes, for instance, grazing-sliding of a limit cycle shown in Fig. 1.3(i).

5.2. Sliding bifurcation at a visible fold: crossing case. Orbits that originate in $h < 0$ in the unfolding given by (5.4) behave somewhat differently, shown in Fig. 5.1(ii). We can reparameterize the curve of impact coordinates as $x_0(\mu) = (\mu, -\frac{1}{2}\mu^2, -\frac{1}{2}\mu^2)$, and consider the nongeneric orbit at $\mu = 0$. This is transverse to the

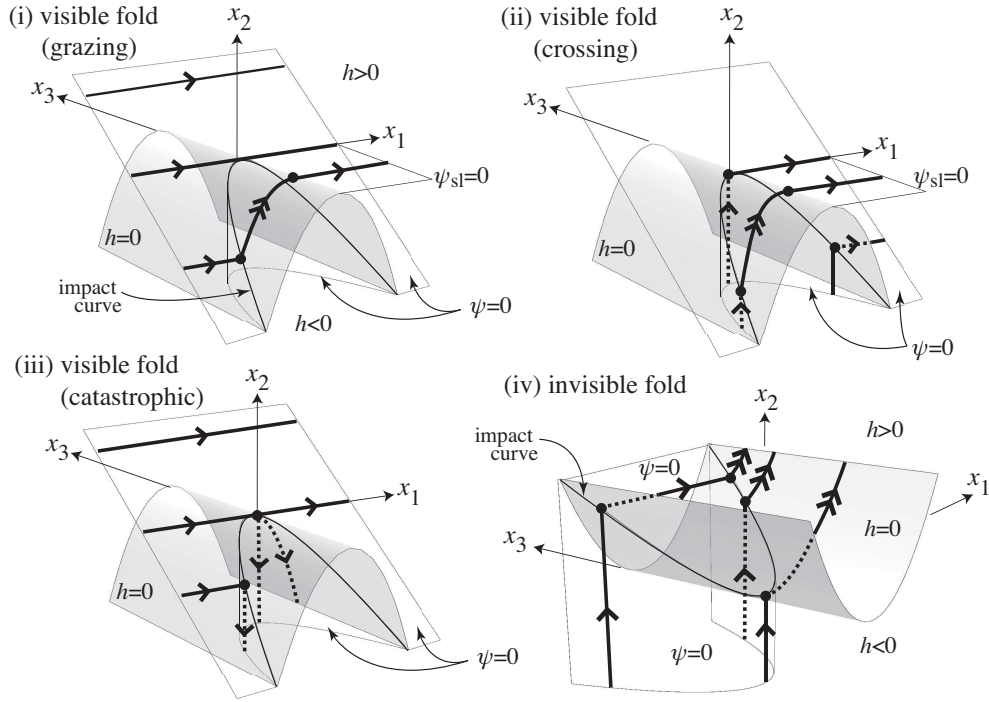


FIG. 5.1. Sliding bifurcation at a fold. The switching manifold is the shaded surface $h = x_2 \pm \frac{1}{2}x_1^2 = 0$. A nongeneric orbit intersects the origin. Its unfolding is $\psi = 0$, with sliding separatrix $\psi_{sl} = 0$ (in (i-ii) only). The sliding bifurcations are classified as: (i) at a visible fold (grazing case), where the nongeneric orbit visibly grazes at the boundary of stable sliding; (ii) at a visible fold (crossing case), where the nongeneric orbit crosses the manifold at the boundary of stable sliding; (iii) at a visible fold (catastrophic case), where the nongeneric orbit splits into grazing, crossing, and sliding solutions at the boundary of unstable sliding; (iv) at an invisible fold, where the nongeneric orbit hits the fold transversally. Arrows can be reversed in each case to obtain the same four phase portraits with the opposite stability of sliding.

switching manifold, but it intersects the fold from $h < 0$, implying a different sliding bifurcation to section 5.1. On one side of the bifurcation, $\mu > 0$, the orbit crosses the manifold. On the other side, $\mu < 0$, the orbit has a sliding segment connecting the curve $\{x_0(\mu) : \mu < 0\}$ to the fold, and escapes the manifold on the sliding separatrix $\psi_{sl} = 0$ given by (5.5). We call this the *crossing case* of the sliding bifurcation at a visible fold. See Fig. 6.1.2 for its illustration at a flat switching manifold. It describes, for instance, crossing-sliding of a limit cycle shown in Fig. 1.3(ii).

5.3. Sliding bifurcation at a visible fold: catastrophic case. If we reverse the time direction for $h < 0$ in the system (3.1), so that $\mathcal{L}_f - h < 0$, and keep the same unfolding from (5.4), then orbits originating in $h > 0$ undergo a discontinuous change as they pass through grazing, shown in Fig. 5.1(iii).

As for the grazing case, section 5.1, we can label orbits by parameterizing the impact coordinates as $x_0(\mu) = (\pm\sqrt{-2\mu}, \mu, \mu)$. The nongeneric orbit at $\mu = 0$ grazes the manifold. When it grazes, the solution becomes non-unique, since it can remain in $h > 0$ as a smooth orbit, or cross through to $h < 0$, or enter the unstable sliding region; all three are shown in Fig. 5.1(iii).

For $\mu > 0$ the orbit is smooth, lies in $h > 0$, and does not impact the manifold.

For $\mu < 0$, the orbit crosses the manifold on the curve $x_0(\mu) = (-\sqrt{-2\mu}, \mu, \mu)$, and the outgoing trajectory crosses to $h < 0$. This is the *catastrophic case* of the sliding bifurcation at a visible fold. The phase portrait is not equivalent to either the grazing or crossing cases from section 5.1-5.2. The sliding bifurcation is catastrophic in the sense that perturbing the grazing orbit causes a discontinuous change in its outset from the neighbourhood of the fold, while its inset changes continuously. See Fig. 6.1.5 for its illustration at a flat switching manifold.

This sliding bifurcation describes, for instance, the catastrophic destruction of a limit cycle by grazing-sliding. As a catastrophic event, it is qualitatively different from the sliding bifurcations in sections 5.1-5.2, and those in 5.4-5.5 which follow, yet it arises naturally in our classification. It has been suggested before from numerical simulations (section 8.6.1 of [6]) where it is referred to as “catastrophic grazing-sliding”. It has since been observed in a model of a superconducting resonator [15], which to our knowledge is the first time it has been identified in experiments.

By inspection, sections 5.1-5.3 exhaust the possible sliding bifurcations of orbits in the unfolding given by (5.4). Reversing the arrow of time reverses the stability of sliding but, up to time direction, all cases are equivalent to the three described above.

5.4. Sliding bifurcation at an invisible fold. Consider the system given by taking $h(x) = x_2 - \frac{1}{2}x_1^2$ from (4.1), with the straightened vector field of (3.1). By Definition 2.1.2 this describes an invisible fold. We treat this similarly to the visible fold, again setting $\rho = x_3$ in (5.1). Hence we find that an unfolding of the *sliding bifurcation at an invisible fold* is given by $\psi = 0$, where

$$\begin{aligned} \psi(x) &= x_3 - x_2 + h(x)\Theta[-h(x)], \\ \text{and} \quad h(x) &= x_2 - \frac{1}{2}x_1^2. \end{aligned} \tag{5.6}$$

This is shown in Fig. 5.1(iv). We will now describe this figure.

The sliding region on $h = 0$ is in $x_1 > 0$, and sliding segments flow away from the fold. Orbits impact the manifold on the curve $x_0(\mu) = (\mu, \frac{1}{2}\mu^2, \frac{1}{2}\mu^2)$, and we can label orbits by μ . Every orbit near an invisible fold must cross the manifold and hence has an impact coordinate. At $\mu = 0$ a nongeneric orbit hits the fold, implying a sliding bifurcation. This orbit hits the manifold transversally from $h < 0$, then slides. For $\mu > 0$, orbits impact the manifold from below and then slide. For $\mu < 0$, orbits cross the manifold into $h > 0$, then impact again at $x_1 = -\mu$ and slide. See Fig. 6.1.3 for the illustration of this at a flat switching manifold. It describes, for example, switching-sliding of a limit cycle shown in Fig. 1.3 (iii).

The case with unstable sliding is found by reversing time in (3.1), but by inspection, up to time reversal, no sliding bifurcations other than Fig. 5.1(iv) are possible. So far we have shown that three of the known sliding bifurcations (grazing-sliding, crossing-sliding and switching-sliding in Fig. 1.3) and a new one (catastrophic grazing-sliding) take place at a fold. In the next section we show that the only other previously known sliding bifurcation, adding-sliding in Fig. 1.3(iv), takes place at a cusp.

5.5. Sliding bifurcation at a visible cusp. Now consider the vector field in (3.1) with the switching manifold $h(x) = x_2 + \frac{1}{3}x_1^3 + x_3x_1 = 0$ from (4.2). By Definition 2.2, this has a cusp at the origin. From (5.1), the unfolding is the surface $\psi = 0$ where

$$\begin{aligned} \psi(x) &= \rho(x_3) - x_2 + h(x)\Theta[-h(x)], \\ \text{and} \quad h(x) &= x_2 + \frac{1}{3}x_1^3 + x_3x_1, \end{aligned} \tag{5.7}$$

shown in Fig. 5.2. Solving (5.2), we find that the impact coordinates satisfy $\rho(x_3) = x_2 = -\frac{1}{3}x_1^3 - x_3x_1$. Hence we can parameterize the impact coordinates as

$$x_0(\mu_1, \mu_2) = (\mu_1, -\frac{1}{3}\mu_1^3 - \mu_1\mu_2, \mu_2). \quad (5.8)$$

Since x_3 is constant along the flow, substituting $\rho = -\frac{1}{3}\mu_1^3 - \mu_1\mu_2$ into (5.7) gives

$$\psi(x) = \frac{1}{3}(x_1 - \mu_1)(x_1^2 + x_1\mu_1 + \mu_1^2 + 3\mu_2) - h(x)\Theta[h(x)]. \quad (5.9)$$

Because this requires two parameters, μ_1 and μ_2 , an orbit at the cusp has a two-parameter unfolding. This means that a one-parameter family of orbits does not generically intersect the cusp directly from $h > 0$ or $h < 0$.

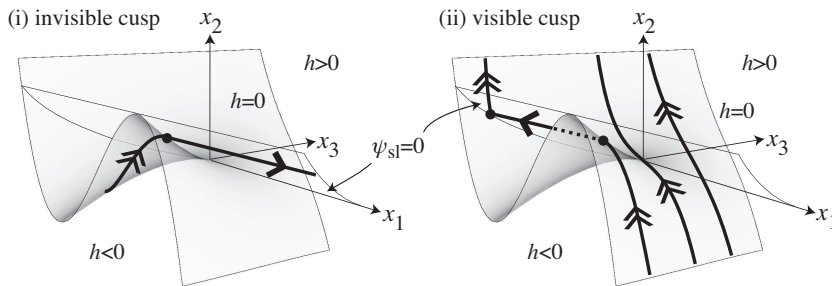


FIG. 5.2. The cusp, with switching manifold $h = x_2 + \frac{1}{3}x_1^3 + x_3x_1 = 0$ and sliding separatrix $\psi_{sl} = 0$ given by (5.10). Sliding segments are shown with double arrows. (i) At the invisible cusp the sliding region is $h = 0$, $x_3 < -x_1^2$. (ii) At the visible cusp the sliding region is $h = 0$, $x_3 > -x_1^2$. The vector field in $h < 0$ is vertically upward for stable sliding; reverse arrows for unstable sliding.

Curves of fold points branch from the origin: a visible fold along $x = x_0(\sqrt{-\mu_2}, \mu_2)$ and an invisible fold along $x = x_0(-\sqrt{-\mu_2}, \mu_2)$, for $\mu_2 < 0$. The separatrix between sliding and crossing dynamics is the surface $\psi_{sl} = 0$ whose impact coordinates lie along a visible fold where $\mu_1 = \sqrt{-\mu_2}$, which is therefore given by

$$\psi_{sl} = \frac{1}{3}(x_1 - \sqrt{-\mu_2})^2(x_1 + 2\sqrt{-\mu_2}) - h(x)\Theta[h(x)]. \quad (5.10)$$

As shown in Fig. 5.2, orbits in a stable sliding region flow towards the visible fold, then escape the switching manifold within the sliding separatrix. By Definition 2.2 there are two cases to consider. The system in (3.1) gives an invisible cusp, since $(\mathcal{L}_{f^+}^3 h)(\mathcal{L}_f - h) > 0$. This has sliding segments only for $\mu_2 < 0$ (or $x_3 < 0$, $h = 0$) and is shown in Fig. 5.2(i). Furthermore, the sliding segment tangent to the cusp consists of only a single point, and therefore cannot give rise to sliding bifurcations.

If we reverse the time direction in $h > 0$ of (3.1) so that $(\mathcal{L}_{f^+}^3 h)(\mathcal{L}_f - h) < 0$, we obtain the visible cusp as shown in Fig. 5.2(ii). In this case there is a nongeneric sliding segment with a visible tangency to the sliding boundary at the cusp (recall Fig. 1.2(iii) for the definition of a visible tangency). This means that a one-parameter sliding bifurcation can occur, and its unfolding is given by the separatrix $\psi_{sl} = 0$ combined with sliding segments on $h = 0$. Since (5.10) has only one parameter, μ_2 , it defines a one-parameter unfolding for the *sliding bifurcation at a visible cusp*.

Reversing the overall time direction, we obtain visible and invisible cusps with unstable sliding. The phase portraits are the same as the stable cases up to time direction, so the only distinct one-parameter sliding bifurcation at a cusp is the visible case, Fig. 5.2(ii). This is illustrated at a flat switching manifold in Fig. 6.1.4. An example of it is adding-sliding of a limit cycle, shown in Fig. 1.3.

By considering the map $(\mu_1, \mu_2) \mapsto x_0(\mu_1, \mu_2)$ from (5.8), we can obtain the bifurcation diagram for sliding bifurcations near a cusp shown in Fig. 5.3. Sliding bifurcations at a fold take place at the visible fold (V) or the invisible fold (I), and degenerate combinations occur at the cusp. The separatrix from (5.10) impacts the switching manifold along the curve $\mu_2 = -\mu_1^2/4$ (R).

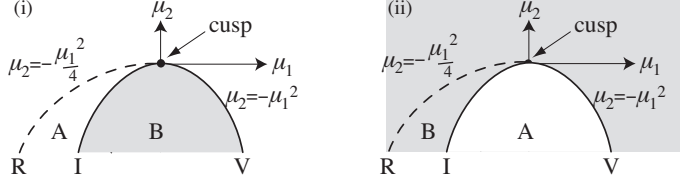


FIG. 5.3. Bifurcation curves in parameter space (μ_1, μ_2) for: (i) the invisible cusp, and (ii) the visible cusp. Visible (V) and invisible (I) fold branches separate sliding (shaded) and crossing (unshaded). Grazing orbits impact along R. The flow in $h > 0$ maps points from region A to B.

If we return to (5.7), we can obtain a typical unfolding by letting $\rho(x_3) = \rho_1 + \rho_2 x_3$, where ρ_1 and ρ_2 are constants that respectively specify the height and angle, with respect to the switching manifold, of a family of orbits parameterized by x_3 . Such a surface has four topologically different forms, depending on the signs of the quantities ρ_1 and $\rho_1 - \frac{1}{3}\rho_2^3$: the unfolding contains one visible grazing orbit if $\rho_1 < 0$ and one invisible grazing orbit if $\rho_1 > 0$, and three grazing orbits in total if $\rho_1(\rho_1 - \frac{1}{3}\rho_2^3) < 0$. These are shown in Fig. 5.4. They unfold the generic series of sliding bifurcations that will be observed by one-parameter variation of an orbit near a cusp, including all possible sliding bifurcations at the folds.

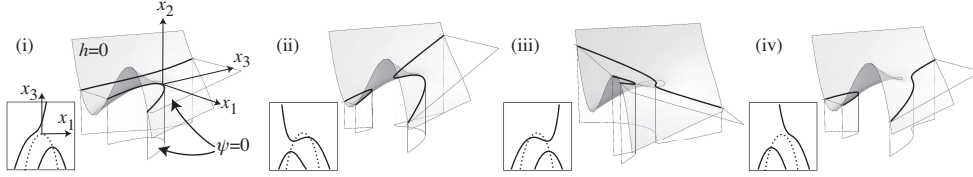


FIG. 5.4. The family of unfoldings from (5.7), with: (i) $\rho_1 > 0$ and $\rho_1 - \rho_2^3/3 > 0$, (ii) $\rho_1 > 0$ and $\rho_1 - \rho_2^3/3 < 0$, (iii) $\rho_1 < 0$ and $\rho_1 - \rho_2^3/3 > 0$, (iv) $\rho_1 < 0$ and $\rho_1 - \rho_2^3/3 < 0$. The intersections $h = \psi = 0$ are depicted inset, and have turning points along the folds (dotted).

An example of a one-parameter unfolding is shown in Fig. 5.5, showing the same surface unfolding orbits around a cusp whether it is visible (i-iii) or invisible (iv).

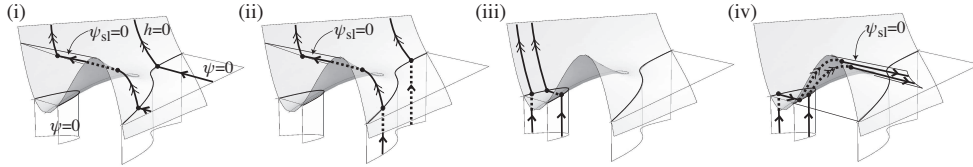


FIG. 5.5. An example of the unfoldings from (5.7), with $\rho_1 < 0$ and $\rho_1 < \rho_2^3/3$. (i-iii) show a visible cusp, (iv) shows an invisible cusp. These exhibit sliding bifurcations: (i-ii) at a visible cusp (from Fig. 5.2(ii)), (iii-iv) at an invisible fold (from Fig. 5.1(iv)). Sliding orbits escape on the separatrix $\psi_{sl} = 0$. Stable sliding cases are shown, simply reverse arrows for unstable sliding.

5.6. Catastrophic sliding bifurcations at a two-fold. Up to now we have seen four sliding bifurcations in which an orbit changes continuously, but nondifferentiably, and one catastrophic case where the orbit changes discontinuously. In this section we show that there are three further sliding bifurcations that are catastrophic in nature, hitherto unclassified, and all originating from the two-fold.

Consider the vector field in (3.1), with the switching manifold $h(x) = x_3 + \frac{1}{2}\alpha x_1^2 - \frac{1}{2}\beta x_2^2 + x_1 x_2 = 0$ from (4.3). If the Hessian determinant over x_1, x_2 , given by $(\partial^2 h / \partial x_1^2)(\partial^2 h / \partial x_2^2) - (\partial^2 h / \partial x_1 \partial x_2)^2 = -(1 + \alpha\beta)$, is negative then the manifold is a saddle, if it is positive then the manifold is a bowl (similar to Fig. 5.7).

Because the two-fold consists of tangencies to both sides of the manifold, the constant g in (5.3) is 1. Hence, by (5.1), the unfolding $\psi = 0$ is given by

$$\begin{aligned} \psi(x) &= \rho(x_3) - x_3, \\ \text{and } h(x) &= x_3 + \frac{1}{2}\alpha x_1^2 - \frac{1}{2}\beta x_2^2 + x_1 x_2. \end{aligned} \quad (5.11)$$

By (5.2), impact coordinates satisfy $\rho(x_3) = x_3 = -\frac{1}{2}\alpha x_1^2 + \frac{1}{2}\beta x_2^2 - x_1 x_2$, and can be parameterized as

$$x_0(\mu_1, \mu_2) = (\mu_1, \mu_2, -\frac{1}{2}\alpha\mu_1^2 + \frac{1}{2}\beta\mu_2^2 - \mu_1\mu_2). \quad (5.12)$$

The folds lie along $\mathcal{L}_{f^+}h = \alpha\mu_1 + \mu_2 = 0$ and $\mathcal{L}_{f^-}h = \mu_1 - \beta\mu_2 = 0$, with the signs of the second derivatives $\mathcal{L}_{f^+}^2 h = \alpha$ and $\mathcal{L}_{f^-}^2 h = -\beta$ respectively determining whether they are visible or invisible. At a visible fold, orbits escape the switching manifold and form sliding separatrices. By solving $\psi = 0$ so that its impact coordinates lie along a fold, we find that the sliding separatrices are given by $\psi_{\text{sl}} = 0$, where

$$\psi_{\text{sl}} = -x_3 + \frac{1 + \alpha\beta}{2\alpha\beta} \begin{cases} \beta x_2^2 & \text{if } h \geq 0, \\ -\alpha x_1^2 & \text{if } h \leq 0. \end{cases} \quad (5.13)$$

An orbit will not generically hit the two-fold from $h > 0$ or $h < 0$, since this requires that both of the parameters μ_1 and μ_2 vanish. Similarly to the cusp, to find sliding bifurcations we must consider sliding segments.

Without analyzing the sliding vector field f^{sl} in detail, we can use its boundary conditions, (1.4), to infer what forms are topologically possible. These conditions state that the sliding vector field f^{sl} , at a point along a fold, is equal to whichever of f^+ or f^- is tangent the switching manifold at that point. Thus $f^{\text{sl}} = f^+$ where $\mathcal{L}_{f^+}h = \alpha x_1 + x_2 = 0$, and $f^{\text{sl}} = f^-$ where $\mathcal{L}_{f^-}h = x_1 - \beta x_2 = 0$. This implies that f^{sl} points outwards from the stable sliding region at a visible fold, and inwards at an invisible fold. (It does the opposite in the unstable sliding region). Then only the sliding topologies shown in Fig. 5.6 are possible. It is a straightforward exercise to verify this by calculating the sliding vector field explicitly using (1.3). These have been listed before [10, 15, 30], but not considered as the source of sliding bifurcations except for remarks made in [14].

Only the cases in Figs. 5.6 (i), (vi), and (vii) give rise to one-parameter sliding bifurcations. These are the only cases in which a sliding segment not only hits the two-fold, but its intersection with the switching manifold changes under perturbation. (In Fig. 5.6(v) no sliding segments hit the two-fold, in the remaining cases any sliding bifurcations are trivial by Definition 1.3.) The unfoldings are illustrated in Fig. 5.7, found by combining sliding trajectories with the sliding separatrices from (5.13).

Fig. 5.7(i) depicts the *sliding bifurcation at a visible two-fold*. This occurs when $\alpha, \beta > 0$, in which case the Hessian determinant of h over x_1, x_2 , is $-(1 + \alpha\beta) < 0$,

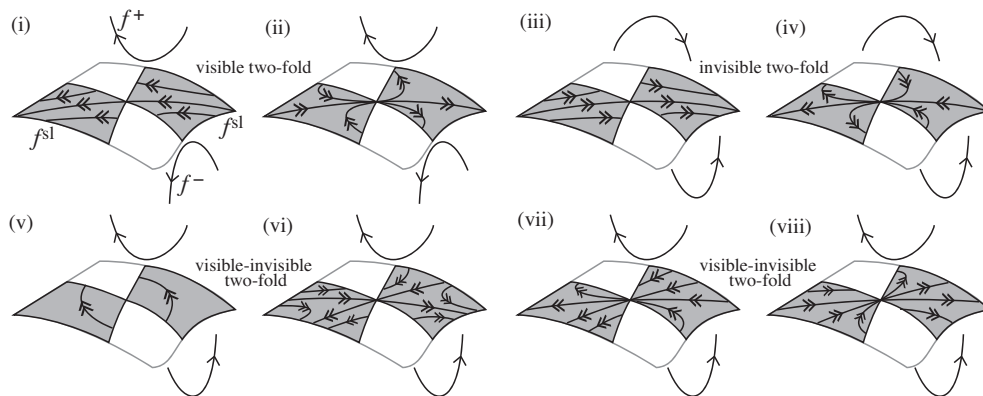


FIG. 5.6. The sliding vector field topologies at the two-folds. Shading regions are shaded. There are two topologies at a visible two-fold (i)-(ii) where $\alpha, \beta < 0$, two at an invisible two-fold (iii)-(iv) where $\alpha, \beta < 0$, and four at a visible-invisible two-fold (v)-(viii) where $\alpha\beta < 0$.

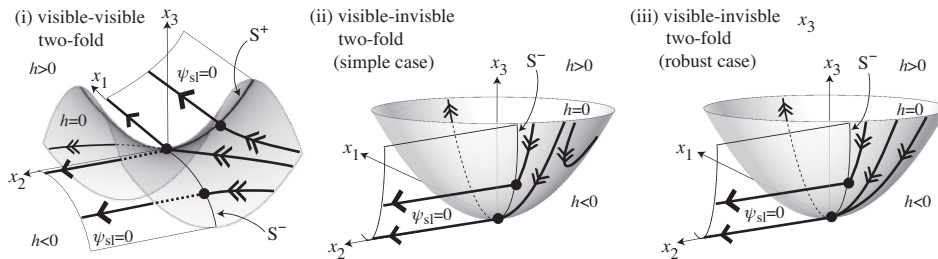


FIG. 5.7. Catastrophic sliding bifurcations at a two-fold for: (i) the visible two-fold; (ii) the visible-invisible two-fold (simple case); (iii) the visible-invisible two-fold (robust case). The stable and unstable sliding regions are bounded by folds marked S^+ where $\alpha x_1 + x_2 = 0$, and S^- where $x_1 - \beta x_2 = 0$, at which orbits escape and form the separatrices $\psi_{sl} = 0$ given by (5.13). At the two-fold singularity the solutions are non-unique, producing orbits that enter the unstable sliding region (canards) and orbits that escape the manifold.

so the switching manifold is a saddle. If the sliding vector field has the form of Fig. 5.6(i), then a nongeneric sliding segment intersects the two-fold. At the two-fold singularity itself the dynamics is non-unique, since both boundary conditions in (1.4) apply there and are contradictory. Thus an orbit may escape into $h > 0$ or $h < 0$, or enter the unstable sliding region as shown. Depending on which way we perturb the nongeneric orbit, we find that an orbit escapes the manifold into either $h > 0$ or $h < 0$, on the sliding separatrix ψ_{sl} given by (5.13).

Figs. 5.7(ii)-(iii) depict the two cases of the *sliding bifurcation at a visible-invisible two-fold*. These can occur if $\alpha\beta < 0$. The switching manifold can be either a saddle or bowl depending on the sign of the Hessian determinant of h ; the figure shows bowls with $-1 - \alpha\beta > 0$. In both cases, a nongeneric sliding segment intersects the two-fold. At the two-fold point the dynamics is non-unique, since orbits can either escape the manifold or enter the unstable sliding region. Perturbing the nongeneric orbit in one direction gives a sliding segment that intersects the visible fold, and escapes $h = 0$ along the sliding separatrix. Perturbing in the opposite direction leads to two possible scenarios. Given the vector field from Fig. 5.6(vi), the orbit will remain locally on the manifold, shown in Fig. 5.7(ii). We call this the *simple case*. Alternatively, given the

vector field from Fig. 5.6(vii), there is a one-parameter family of orbits that intersects the two-fold, shown in Fig. 5.7(iii). Here the intersection with the singularity persists and we call this the *robust* case.

Sliding orbits that pass through the two-fold point are ‘canards’ as defined in [27] – trajectories that pass from stable to unstable invariant manifolds (sliding regions). In Figs. 5.7(i-ii), the only canard is the nongeneric orbit, while in Fig. 5.7(iii) there is a one-parameter family of canards; hence the ‘singular’ and ‘robust’ classification.

In the neighbourhood of an invisible two-fold, given by $\alpha < 0$ and $\beta < 0$, orbits map repeatedly back onto the switching manifold. This case is interesting in its own right and has been extensively studied in [10, 13, 29]. The unfoldings $\psi = 0$, given by (5.11), form invariant surfaces around which orbits rotate until they impact and slide. These are associated with local bifurcations studied in [16], but the invisible two-fold does not produce any sliding bifurcations.

5.7. Completeness of the classification. A general switching manifold may contain any number of the singularities we have studied. Their genericity, however, means that when any singularity is perturbed it will degenerate into folds. The sliding bifurcations are generic in the sense that any system can be perturbed to one exhibiting only those listed in Table 5.1 below.

Sliding bifurcation:	Figure:
1. at a visible fold, grazing case	Fig. 5.1(i)
2. at a visible fold, crossing case	Fig. 5.1(ii)
3. at an invisible fold	Fig. 5.1(iv)
4. at a visible cusp	Fig. 5.2(ii)
5. at a visible fold, catastrophic case	Fig. 5.1(iii)
6. at a visible two-fold	Fig. 5.7(i)
7. at a visible-invisible two-fold, simple case	Fig. 5.7(ii)
8. at a visible-invisible two-fold, robust case	Fig. 5.7(iii)

TABLE 5.1

The eight one-parameter sliding bifurcations. The catastrophic cases are 5-8.

To prove that this classification is complete is a rather straightforward exercise. We consider what singularities will generically be hit (intersected) by orbits, either individually or in one-parameter families. Recall from Definition 1.1 that a generic orbit is a concatenation of generic trajectories of (1.2) and of (1.3), and that a singularity is a point where, without loss of generality, $\mathcal{L}_{f^+}h = h = 0$. Then we have:

LEMMA 5.1. *If an orbit of (1.2)-(1.3) in \mathbb{R}^n , for $n \geq 2$, hits a singularity, the singularity is generically a fold.*

Proof. This is an immediate consequence of the fact that orbits can generically contain sliding segments, which are one dimensional curves on the switching manifold, and the fold is the only codimension one singularity of $h = 0$, provided that, at the singularity, $\mathcal{L}_{f^+}^2h(x^*) \neq 0$ and $\mathcal{L}_{f^-}h(x^*) \neq 0$ (definition 2.1). \square

LEMMA 5.2. *If a one-parameter family of orbits of (1.2)-(1.3) in \mathbb{R}^n , for $n \geq 3$, hits a singularity, the singularity is generically a fold, a cusp, or a two-fold.*

Proof. From Lemma 5.1, an orbit with a sliding segment may generically hit a fold, but will miss singularities of higher codimension. However, the intersection of a one-parameter family of orbits with a fold is a one-dimensional curve. Since a cusp or two-fold occurs at an isolated codimension one set in the locus of folds, it can occur generically along such a one-dimensional intersection, and hence be hit by a one-parameter family of orbits. Then consider a higher codimension singularity. This

is a codimension r set in a locus of folds with $r > 1$. It therefore does not occur generically in the one-dimensional intersection between a fold and a one-parameter family of orbits. This result is independent of the number of dimensions, provided that $n \geq 3$ so the fold, cusp, and two-fold occur generically, and therefore the lemma holds in \mathbb{R}^n for $n \geq 3$. \square

We therefore have the central result of this paper:

THEOREM 1.4 *A generic one-parameter sliding bifurcation in \mathbb{R}^n for any $n \geq 3$ is a sliding bifurcation at a fold, a cusp, or a two-fold.*

Proof. A generic one-parameter sliding bifurcation takes place at a tangency between the vector field and the switching manifold, which corresponds to a singularity where $\mathcal{L}_{f+h} = h = 0$. Its unfolding is a one-parameter family of orbits, which, by Lemma 5.2, may generically hit a fold, a cusp, or a two-fold, but not a higher codimension singularity. \square

If the derivatives that define a fold, cusp, or two-fold, vanish, but the nondegeneracy conditions given in Definitions 2.1-2.3 are violated, then the singularity they define has a higher codimension. Higher codimension singularities can be derived from section 4 with V taking the form of swallowtail and butterfly catastrophe manifolds [24], or by taking intersections of folds with cusps/two-folds, and so on. Lemma 5.2 implies that for an orbit to hit these requires at least two parameters. We discuss these briefly in the next section.

5.8. Two-parameter sliding bifurcations. Surfaces $\psi = 0$ of the form given by (5.1) can also be used to describe unfoldings of higher codimension sliding bifurcations. Consider the cusp or two-fold. An orbit that hits the cusp from $h > 0$ or $h < 0$ has the form $0 = \frac{1}{3}x_1^3 + h\Theta[h]$, $x_3 = 0$ (see (5.7)). By varying the two parameters μ_1 and μ_2 we obtain a two-parameter unfolding. This codimension two scenario has been described in [17] for a visible or invisible cusp with stable sliding. Similarly, an orbit that hits the two-fold from $h > 0$ or $h < 0$ can be reached only by control of two parameters in the unfolding from (5.11). This has not been considered before in the literature on sliding bifurcations. By varying x_3 and either μ_1 or μ_2 , we obtain a two-parameter unfolding.

Also among the two-parameter sliding bifurcations are cases where a sliding segment intersects a codimension 3 singularity. We can refer to singularity theory, as in section 4, to find that for the piecewise-straightened vector fields in (3.1), the switching manifold $h = 0$ can take the form of: the swallowtail $h = x_2 + (\frac{1}{4}x_1^4 + \frac{1}{2}x_3x_1^2 + x_4x_1)$, the lips $h = x_2 + (\frac{1}{3}x_1^3 + (x_3^2 + x_4)x_1)$ or beak-to-beak $h = x_2 + (\frac{1}{3}x_1^3 - (x_3^2 + x_4)x_1)$, and the fold-cusp $h = x_4 + (\frac{1}{3}x_1^3 + x_3x_1 + \frac{1}{2}x_2^2)$, where “ $\pm\frac{1}{2}x_2^2$ ” is a Morse term similar to that which describes a fold.

In every case, two-parameter sliding bifurcations take place at singularities that arise as subsets along the locus of folds, cusps, and two-folds. They are therefore comprised of degenerate combinations of the eight one-parameter sliding bifurcations introduced in section 5.

6. Concluding remarks. By considering a piecewise-straight vector field with a curved switching manifold, we have studied the geometry that gives rise to sliding bifurcations. We have thus found that eight sliding bifurcations can occur as one parameter is varied in a generic Filippov system. They can be divided into two types: the regular sliding bifurcations 1-4 in Table 5.1, in which an orbit changes continuously and remains unique; and the catastrophic sliding bifurcations 5-8 in Table 5.1, in which an orbit changes discontinuously, and is non-unique at the bifurcation itself.

This paper aims to provide a foothold for a bifurcation theory of piecewise-smooth systems that is as yet in its infancy. We have singled out the geometry of discontinuity induced bifurcations in sliding systems, focusing on the singularities and bifurcations that arise through loss of transversality between a vector field and a switching manifold. To these fundamentals we must add bifurcations on switching manifolds that have self-intersections or corners, and bifurcations of equilibria or invariant manifolds. The study of these for dimension $n > 2$ has barely begun.

It is worth re-emphasising that sliding bifurcations are *global* bifurcations (Fig. 1.4). They affect global sets (limit cycles, stable manifolds, etc) that graze the switching manifold, but the bifurcation relies only on the geometry in the neighbourhood of grazing. Global conditions give orbits in the unfolding a specific identity. A sliding bifurcation can be viewed locally as a bifurcation of orbits with no actual bifurcation of the underlying vector field.

The catastrophic sliding bifurcations are characterized as perturbations of orbits that impact a boundary of unstable sliding. Interpreted as the piecewise-smooth limit of a regularized vector field [31], the non-uniqueness of solutions at the bifurcation can be interpreted as a cascade of orbits that penetrate the unstable sliding region. Far from being a pathological result of nonsmoothness, they are a common feature of real world models. They occur in singular perturbation problems such as the van der Pol system with relation to canards and relaxation oscillations [5, 12, 18], where the sliding vector field is comparable to the ‘reduced’ (or slow) subsystem. They have also been proposed as the mechanism for sudden temperature oscillations observed in superconducting resonators [15, 25], and have been shown to be generic in switched feedback controllers [4].

A truly pathological feature of Filippov systems is the nondeterminism faced where both vector fields are tangent to the switching manifold (the two-fold, fold-cusp, etc). This presents an ongoing dilemma for the interpretation of piecewise-smooth models, particularly since, in the sliding bifurcation at a visible-invisible two-fold (Fig. 5.7(ii)), a limit cycle can jump instantly from sliding to robust nondeterministic behaviour. The resolution is likely to lie in closer study of the sliding bifurcations at two-folds in models of real world systems.

Appendix: Normal forms at a flat switching manifold. Given the piecewise-constant vector field in (3.1) and normal forms for singularities of the switching manifold in section 4, we now find coordinates in which the switching manifold is flat (and the vector field is no longer straight). These are more common in the literature on piecewise-smooth systems, and therefore useful for illustration.

Given a manifold written locally in the form $h(x) = x_i + V(x)$ as in (4.1)-(4.3), we make the smooth transformation to coordinates $y = (y_1, y_2, y_3)$ in which the switching manifold is given by $y_i = 0$. The unfolding function (5.1) is then given by $\psi(y) = \rho(y_3) + V(y) - y_i g(y)$. We now demonstrate the transformation for each of the singularities in Definitions 2.1-2.3.

Near the fold, section 5.1, a transformation to $(y_1, y_2, y_3) = (x_1, h, x_3)$ gives

$$(\dot{y}_1, \dot{y}_2, \dot{y}_3) = \begin{cases} (1, \pm y_1, 0) & \text{if } y_2 > 0, \\ (0, 1, 0) & \text{if } y_2 < 0. \end{cases} \quad (6.1)$$

Sliding bifurcations at a fold in these coordinates are shown in Figs. 6.1 parts 1,2,3,5.

Near the cusp in section 5.5, a transformation to $(y_1, y_2, y_3) = (x_1, h, x_3)$ gives

$$(\dot{y}_1, \dot{y}_2, \dot{y}_3) = \begin{cases} (1, y_1^2 + y_3, 0) & \text{if } y_2 > 0, \\ (0, 1, 0) & \text{if } y_2 < 0. \end{cases} \quad (6.2)$$

The sliding bifurcation at a visible cusp is shown in Fig. 6.1.4.

Near the two-fold in section 5.6 we transform to $(y_1, y_2, y_3) = (x_1, x_2, \gamma h)$, where γ is a scaling constant that can take different values either side of the switching manifold. A similar constant at the fold or cusp has no topological effect, but at the two-fold it must be included for the sliding vector field to realise all of the topologies in Fig. 5.6. Without loss of generality we can let $\gamma = 1$ for $h > 0$, and let $\gamma = \gamma^-$ for $h < 0$. Then the two-fold vector field near a flat switching manifold is given by

$$(\dot{y}_1, \dot{y}_2, \dot{y}_3) = \begin{cases} (1, 0, \alpha y_1 + y_2) & \text{if } y_3 > 0, \\ (0, 1, (y_1 - \beta y_2)\gamma^-) & \text{if } y_3 < 0. \end{cases} \quad (6.3)$$

The sliding bifurcations at a two-fold then are shown in Fig. 6.1 parts 6-8.

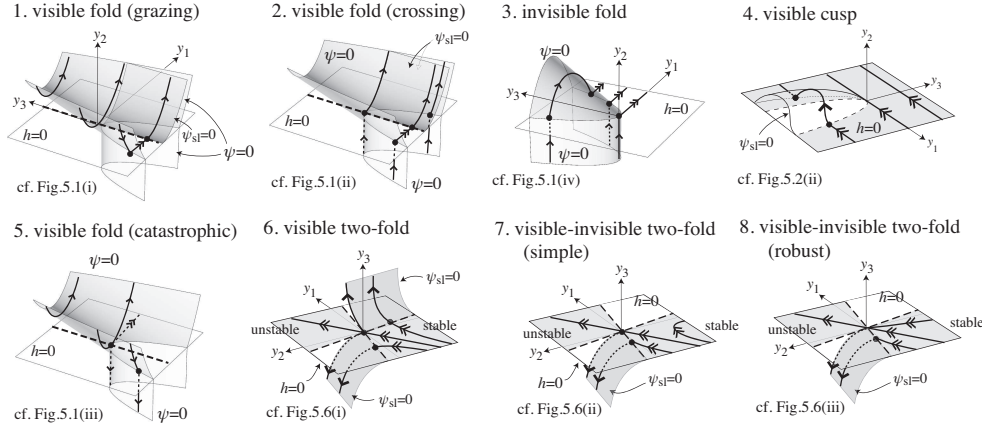


FIG. 6.1. The eight generic one-parameter sliding bifurcations, shown in coordinates where the switching manifold $h = 0$ is flat. The labels 1-8 correspond to the classification in Table 5.1. The surface $\psi = 0$ is the unfolding. Sliding segments are shown with double arrows, and leave $h = 0$ on the sliding separatrix $\psi_{sl} = 0$.

The piecewise-smooth vector fields in (6.1-6.3), are equivalent to normal forms defined by previous authors, up to coordinate transformations that are linear in $h > 0$ and $h < 0$, and continuous at $h = 0$. The fold, cusp, and two-folds all appear in the seminal work by Filippov [10], with local vector fields similar to (6.1-6.3). Normal forms have since been derived for each of these. The cusp follows directly from the cusp at the boundary of a manifold given in [26]. Teixeira’s normal forms for two-folds [29, 30] are obtained from (6.3) by letting $(x, y, z) = (y_1 + \alpha^{-1}y_2, (y_1 - \beta y_2)\gamma^-, y_3)$, then f^+ is notated in [29, 30] as $X(x, y, z) = (1, \gamma^-, x)$ and f^- as $Y(x, y, z) = (\alpha^{-1}, -\beta\gamma^-, y)$, in terms of the parameters α, β, γ^- [this excludes Teixeira’s case “a5” where the vector fields are not everywhere transverse].

The cusp is also equivalent to the codimension one “double tangency”, studied in planar Filippov systems in [20]. There, a parameter (called α) replaces the coordinate y_3 in (6.3) (which is valid since $\dot{y}_3 = 0$). The two-folds are referred to as “collisions of tangencies”, but in this case the vector fields are not equivalent, since the two-fold requires at least 3 dimensions to express generically.

Acknowledgements. The authors wish to thank D. Chillingworth for many helpful discussions, and J. Guckenheimer and P. Holmes for comments on earlier drafts of this work.

REFERENCES

- [1] M. E. BROUCKE, C. PUGH, AND S. SIMIC, *Structural stability of piecewise smooth systems*, Computational and Applied Mathematics, 20 (2001), pp. 51–90.
- [2] J. W. BRUCE AND P. J. GIBLIN, *Curves and Singularities*, Cambridge University Press, 1984.
- [3] D. R. J. CHILLINGWORTH, *Differential topology with a view to applications*, Pitman, 1976.
- [4] A. COLOMBO, M. DI BERNARDO, E. FOSSAS, AND M. R. JEFFREY, *Teixeira singularities in 3D switched feedback control systems*, Systems and Control Letters, (accepted July 2010).
- [5] M. DESROCHES, B. KRAUSKOPF, AND H. M. OSINGA, *Mixed-mode oscillations and slow manifolds in the self-coupled Fitzhugh-Nagumo system*, Chaos, 18 (2008), p. 015107.
- [6] M. DI BERNARDO, C. J. BUDD, A. R. CHAMPNEYS, AND P. KOWALCZYK, *Piecewise-Smooth Dynamical Systems: Theory and Applications*, Springer, 2008.
- [7] M. DI BERNARDO, F. GAROFALO, L. GLIELMO, AND F. VASCA, *Switchings, bifurcations, and chaos in dc/dc converters*, IEEE Trans. Circuits Syst. I, 45 (1998), pp. 133–141.
- [8] M. DI BERNARDO, P. KOWALCZYK, AND A. NORDMARK, *Bifurcations of dynamical systems with sliding: derivation of normal-form mappings*, Physica D, 170 (2002), pp. 175–205.
- [9] M. I. FEIGIN, *Forced Oscillations in Systems with Discontinuous Nonlinearities*, Nauka, Moscow. (In Russian), 1994.
- [10] A. F. FILIPPOV, *Differential Equations with Discontinuous Righthand Sides*, Kluwer Academic Publishers, Dordrecht, 1998.
- [11] M. GOLUBITSKY AND D. G. SCHAEFFER, *Singularities and groups in bifurcation theory*, vol. 1 of Applied Mathematical Sciences 51, Springer-Verlag, 1984.
- [12] J. GUCKENHEIMER, K. HOFFMAN, AND W. WECKESSER, *The forced van der Pol equation I: the slow flow and its bifurcations*, SIAM J. App. Dyn. Sys., 2 (2002), pp. 1–35.
- [13] E. A. JACKSON, *Perspectives of Nonlinear Dynamics*, vol. 1, Cambridge University Press, 2009.
- [14] M. R. JEFFREY, *Two-folds in nonsmooth dynamical systems*, Proceedings of the 2nd IFAC conf. on Analysis and Control of Chaotic Systems IFAC-PapersOnLine, (2009).
- [15] M. R. JEFFREY, A. R. CHAMPNEYS, M. DI BERNARDO, AND S. W. SHAW, *Catastrophic sliding bifurcations and onset of oscillations in a superconducting resonator*, Phys. Rev. E, 81 (2010), pp. 016213–22.
- [16] M. R. JEFFREY AND A. COLOMBO, *The two-fold singularity of discontinuous vector fields*, SIAM Journal on Applied Dynamical Systems, 8 (2009), pp. 624–640.
- [17] P. KOWALCZYK AND M. DI BERNARDO, *Two parameter degenerate sliding bifurcations in Filippov systems*, Physica D, 204 (2005), pp. 204–229.
- [18] M. KRUPA AND P. SZMOLYAN, *Relaxation oscillation and canard explosion*, J. Differ. Equ., 174 (2001), pp. 312–368.
- [19] Y. A. KUZNETSOV, *Elements of Applied Bifurcation Theory*, Springer, 2nd Ed., 1998.
- [20] YU. A. KUZNETSOV, S. RINALDI, AND A. GRAGNANI, *One-parameter bifurcations in planar Filippov systems*, Int.J.Bif.Chaos, 13 (2003), pp. 2157–2188.
- [21] R. I. LEINE AND N. HENK, *Dynamics and Bifurcations of Non-Smooth Mechanical Systems*, Springer, 2004.
- [22] S. MANCINI, M. A. S. RUAS, AND M. A. TEIXEIRA, *On divergent diagrams of finite codimension*, Cadernos de Matematica, 01 (2000).
- [23] J. PALIS AND W. DE MELO, *Geometric theory of dynamical systems*, Springer-Verlag, 1982.
- [24] T. POSTON AND I. N. STEWART, *Catastrophe theory and its applications*, Dover, 1996.
- [25] E. SEGEV, B. ABDO, O. SHTEMLUCK, AND E. BUKS, *Novel self-sustained modulation in superconducting stripline resonators*, EPL, 78 (2007), p. 57002 (5pp).
- [26] J. SOTOMAYOR AND M. A. TEIXEIRA, *Vector fields near the boundary of a 3-manifold*, Lecture Notes in Mathematics, 1331 (1988), pp. 169–195.
- [27] P. SZMOLYAN AND M. WECHSELBERGER, *Canards in \mathbb{R}^3* , J. Differ. Equ., 177 (2001), pp. 419–453.
- [28] M. A. TEIXEIRA, *On topological stability of divergent diagrams of folds*, Math. Z., 180 (1982), pp. 361–371.
- [29] ———, *Stability conditions for discontinuous vector fields*, J. Differ. Equ., 88 (1990), pp. 15–29.
- [30] ———, *Generic bifurcation of sliding vector fields*, J.Math.Anal.Appl., 176 (1993), pp. 436–457.
- [31] M. A. TEIXEIRA, J. LLIBRE, AND P. R. DA SILVA, *Regularization of discontinuous vector fields on \mathbb{R}^3 via singular perturbation*, J.Dyn.Dif.Equat., 19 (2007), pp. 309–331.
- [32] V. I. UTKIN, *Variable structure systems with sliding modes*, IEEE Trans. Automat. Contr., 22 (1977).
- [33] S. M. VISHIK, *Vector fields near the boundary of a manifold*, Vestnik Moskovskogo Universiteta, Matematika, 27 (1972), pp. 13–19.
- [34] Z. T. ZHUSUBALYEV AND E. MOSEKILDE, *Bifurcations and Chaos in Piecewise-Smooth Dynamical Systems*, Mainland Press, 2003.